

## Coastal Marine Heatwaves Detection in Java Using Satellite and In-situ

Willy Wulansari<sup>1,3\*</sup>, Sugeng Widada<sup>2</sup>, Lilik Maslukah<sup>2</sup>, Anindya Wirasatriya<sup>2</sup>, Titi Sari<sup>3</sup>

<sup>1</sup>Magister Program of Marine Sciences, Faculty of Fisheries and Marine Science, Universitas Diponegoro

<sup>2</sup>Department of Oceanography, Faculty of Fisheries and Marine Science, Universitas Diponegoro

Jl. Prof. Jacob Rais, Tembalang Semarang 50275 Indonesia

<sup>3</sup>Directorate of Marine Meteorology, Indonesian Agency for Meteorology Climatology and Geophysics

Jl. Angkasa I No.2, Kemayoran Jakarta Pusat 10720 Indonesia

Email: willy@bmkg.go.id

### Abstract

Global warming is driving an increase in the frequency and intensity of Marine Heatwaves (MHWs), which have a significant impact on coastal ecosystems. The detection of MHWs in Indonesia's coastal regions remains understudied due to limited long term in-situ data, while satellite products often have a coarse resolution that cannot capture local coastal dynamics. This study addresses this gap by detecting MHWs on the north coast of Java. It evaluates the performance of the Operational Sea Surface Temperature and Ice Analysis (OSTIA) product by comparing it against in-situ data from four Marine Automatic Weather Stations (Patimban, Karimunjawa, Rembang, and Paciran) from 2022–2024. To simulate an operational satellite based approach, MHWs were identified in the in-situ daily minimum temperature records using a climatology and 90<sup>th</sup> percentile threshold derived from the nearest satellite grid point. The statistical comparison reveals spatially variable differences in MHW frequency, duration, and total days between the two data sources. Event matching analysis indicates the best satellite performance at Paciran (Probability of Detection (POD)=0.74, False Alarm Ratio (FAR)=0.13), where most in-situ events were successfully captured. Conversely, the weakest performance was at Rembang (POD=0.43, FAR=0.59), where the satellite missed over half of the MHW days and exhibited a high false alarm rate. These findings demonstrate that significant MHWs occur in coastal regions, phenomena that may not be accurately captured by satellite data alone.

**Keywords:** Marine Heatwaves, North coast of Java , OSTIA, in-situ data, FAR, POD

### INTRODUCTION

The Intergovernmental Panel on Climate Change reported that the global surface temperature has increased by 1.1°C, a key manifestation of climate change. This warming has led to a rise in global extreme events, including rainfall, floods, cyclones, atmospheric heatwaves, and marine heatwaves (MHWs) (Hobday *et al.*, 2018). Heatwaves including atmospheric and marine has been observed worldwide. Specifically, the term “Marine Heatwave” was first used by Pearce (2011) to describe anomalous seawater temperature events that impact marine ecosystems. Quantitatively, they are identified when sea surface temperatures exceed either a fixed, absolute threshold (Frölicher *et al.* 2018) or a seasonally varying threshold (Hobday *et al.*, 2016). Qualitatively, MHWs are defined as discrete and prolonged periods of anomalously warm water in

spesific location (Oliver *et al.*, 2021).

MHWs have significant impacts on marine ecosystems, causing events such as coral bleaching (Chen *et al.*, 2024), damage to seagrass meadows, and mortality in marine mammals (Jones *et al.*, 2018; Oliver *et al.*, 2018; Smale *et al.*, 2019). In addition to their ecological effects, MHWs also influence weather patterns. For example, major MHWs can potentially increase the maximum intensity of tropical cyclones, with one study projecting an increase of up to 35.4% in the North Pacific and Atlantic (Choi *et al.* 2024). MHWs have also been linked to regional climate anomalies, such as the hotter than usual summer observed around northern Japan in 2023 (Sato *et al.*, 2024).

MHW studies have largely focused on the open ocean at global and regional scales, using satellite data with broad spatial and temporal coverage. However, a study by Schlegel *et al.*

(2017) comparing MHW events in nearshore and offshore waters using a combination of satellite and in-situ data found different results. Their study showed that the proportion of nearshore MHW events that co-occurred with offshore events was low (0.20–0.50). This low value indicates that more than half of all coastal MHWs are not solely driven by large scale (mesoscale) ocean warming, but are also significantly influenced by a combination of local coastal processes and their interaction with offshore conditions.

Several studies have investigated MHWs in Indonesian waters, revealing a range of driving mechanisms. For instance, MHW 2015/2016 in the Indian Ocean south of Java have been linked to large scale climate drivers like El Niño (Iskandar *et al.*, 2021). Other studies have highlighted more specific regional mechanisms, such as downwelling Kelvin waves in the southern waters of East Java in 2013 (Maulida *et al.*, 2022) and local atmospheric forcing in the Savu Sea (Beliyana *et al.*, 2022).

While these studies provide valuable insight, they have predominantly relied on satellite data for open ocean and regional seas. Notably, a gap remains in studies that combine satellite and in-situ data to specifically detect and validate MHWs in dynamic coastal environments within Indonesia. Therefore, this study aims to address this gap by

identifying MHWs on the north coast of Java and its adjacent islands, using combined approach of satellite observations and in-situ data from four Marine Automatic Weather Station (MAWS) for the period 2022–2024. In addition this study aims to validate the performance of a high resolution satellite dataset in detecting these coastal events through a direct comparison. This comparative analysis will quantify the satellite's performance in a complex coastal environment and underscore the value of in-situ observations, even with short temporal records, for monitoring MHWs event.

## MATERIALS AND METHODS

This study utilises two types of sea surface temperature (SST) data: satellite data and in-situ data. Satellite data consists of daily SST from the Operational Sea Surface Temperature and Ice Analysis (OSTIA) with a resolution of 0.05° for the Java Sea region (3–7°S, 105.8–118°E) from 1982 to 2024 conducted from Copernicus Marine Environment Monitoring (CMEMS) (Donlon *et al.*, 2012). To create a consistent time series, OSTIA Reprocessed data (January 1982 – May 2022) was combined with OSTIA Near-Real-Time (NRT) data, applying monthly bias corrections calculated from the overlap period (2007–2022). Area of study and in-situ station location shows in Figure 1.

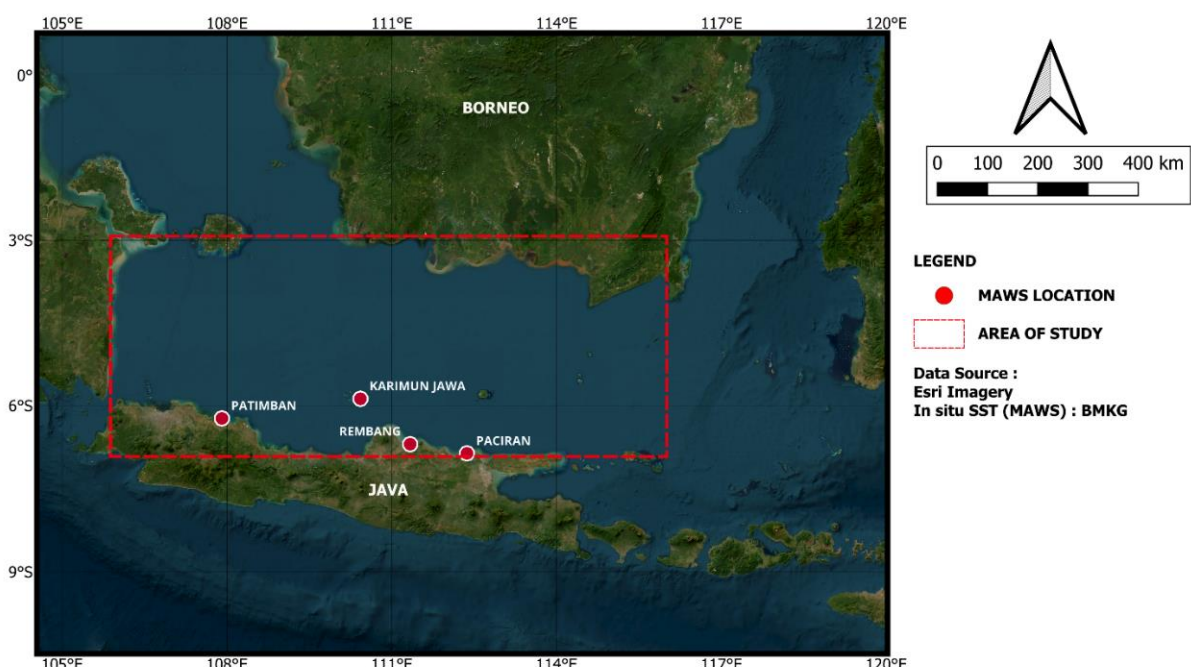


**Figure 1.** Distribution of in-situ data stations within the study area.

In-situ data including sea surface temperature, wind speed, and accumulation of solar radiation were obtained from four Marine Automatic Weather Station (MAWS) stations with hourly resolution: Patimban (September 2022 – December 2024), Rembang (September 2022 – December 2024), Paciran (November 2023 – December 2024), and Karimunjawa (September 2023 - December 2024) (Figure 2). Only data with a quality control flag of 1 (good) was used. These data were obtained from Indonesian Agency for Meteorology, Climatology, and Geophysics (BMKG). To match the OSTIA level 4 of foundation satellite data, which had removed diurnal variations, the sea surface temperature in-situ data analysed was the daily minimum temperature.

Marine Heatwave (MHW) detection follows the definition of (Hobday *et al.* 2016), namely a period of at least five days in which SPL exceeds

the 90th percentile threshold of the reference climatology. Furthermore, two MHW events with a gap of two days or less between them are considered a single, continuous event. Given the limited length of in-situ data, the climatology and thresholds for each station were determined by extracting them directly from the satellite data time series (1982-2024) at the nearest grid point. Standard MHW metrics, including frequency, duration, and intensity, were calculated based on the framework established by Hobday *et al.* (2018) for the in-situ records to compare against the satellite data at these specific locations. In addition to this point based comparison, the spatial characteristics of MHWs including their frequency, maximum intensity, and cumulative days were also calculated for the entire Java Sea using the satellite dataset to provide a broader regional context.

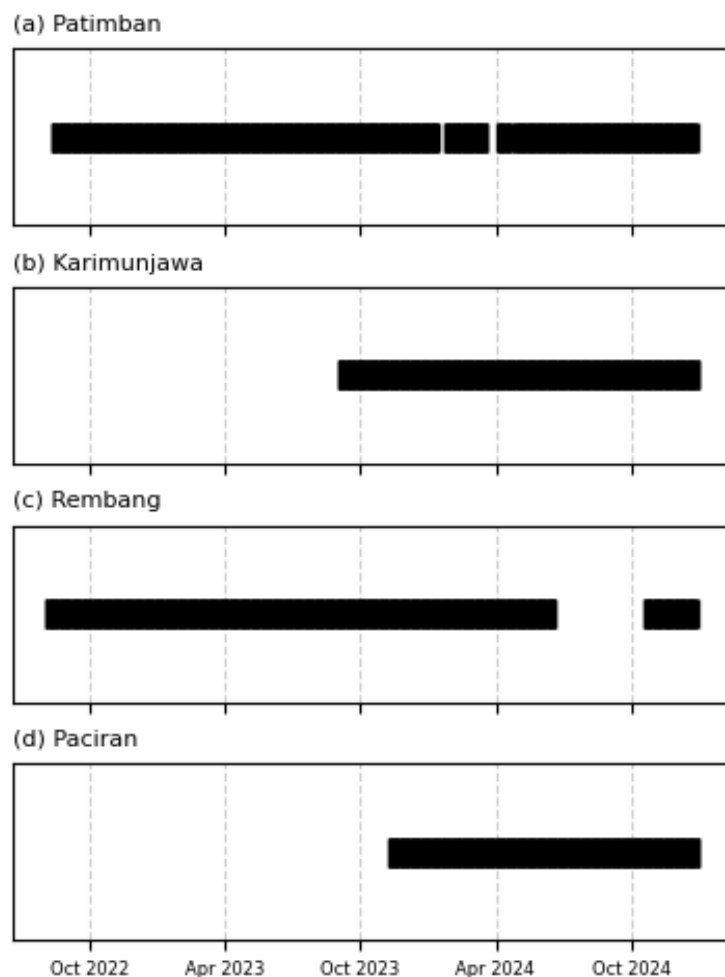


**Figure 2.** The in-situ data availability of MAWS station during 2022-2024 period

To measure the performance of satellite data in replicating MHW events observed by in-situ sensors, we used standard validation metrics, namely Probability of Detection (POD) and False Alarm Ratio (FAR). In this analysis, in-situ data was considered as reference observations, while satellite data was considered as estimates to be validated. The validation metrics POD and FAR refer to (Roebber, 2009) who defined them according to the following equations :

$$POD = \frac{Hits}{Hits + Misses Alarm}$$

$$FAR = \frac{False Alarm}{Hits + False Alarm}$$

A “Hit” occurs if an MHW event is detected in both the in-situ and satellite data. A “Miss” occurs if an MHW is detected by the in-situ data but not by the satellite. A “False Alarm” is when an MHW is detected by the satellite but not in the in-situ data. A high POD value (approaching 1) indicates better performance, as it means the satellite successfully detected most of the events that actually occurred. Conversely, a low FAR value (approaching 0) is better, as it means the satellite rarely produced false alarms for events that did not actually occur.

To identify the drivers of MHWs, further analysis was conducted on three variables. Wind speed and solar radiation was analyzed using the in-situ data from each station, where only data with a quality control flag of 1 (good) were included. Then the diurnal temperature range (DTR) was calculated as the difference between the daily peak time value and the night time SST minimum (Clayson and Weitlich, 2007). DTR found that diurnal forcing from atmospheric variables plays a large role in determining the magnitude of diurnal

warming seen in the skin SST. This DTR variable was used to investigate whether extreme diurnal warming contributed to the formation of MHWs at each location.

## RESULT AND DISCUSSION

The spatial characteristics of MHWs were analyzed for the 2022–2024 period. During this time, the average maximum intensity of MHWs in the Java Sea ranged from 0.8 to 1.8°C. Spatial analysis revealed hotspots with intensities exceeding 1.4°C in the eastern Java Sea (Figure 3a). In contrast, the northern coast of Java consistently exhibited weaker MHW intensities. This difference is likely due to open ocean condition like the hotspot maximum intensity were detected, having a shallower mixed layer and strong stratification, which enhances heat trapping more effectively than in the more dynamic coastal waters (Holbrook *et al.* 2019).

In contrast, the annual frequency of MHW events was higher in coastal regions than in the open ocean. Along the northern coast of Java, the frequency exceeded four events annually. The high frequency in coastal regions is related to local conditions, including shallower waters with a thin mixed layer which allows for faster absorption of atmospheric heat (Schlegel *et al.* 2017). Similarly, the cumulative days per year were longer in the coastal area than in the open sea. This is likely caused by a combination of factors such as shallow sea depth, coastal current, and land-based influences. One significant land-based influence is freshwater runoff, which can create strong stratification at the surface and act as a barrier layer that effectively traps (Mazzini and Pianca, 2022). The primary threat of coastal MHWs is not their peak intensity, which is often lower than offshore events, but their frequency and longer duration. These characteristics create persistent stress on marine biodiversity, fisheries, and coastal tourism.

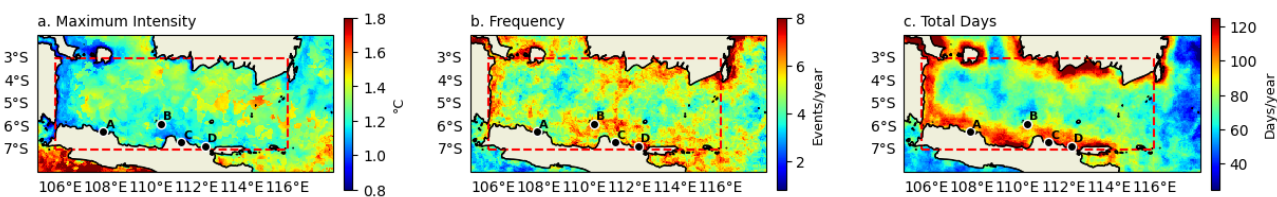


**Figure 3.** Spatial distribution of annual MHW characteristics in the Java Sea (2022-2024) : (a) maximum intensity (°C); (b) frequency (events/year); and (c) cumulative days (days/year). The letters A, B, C, and D on the map indicate the locations of the Patimban, Karimunjawa, Rembang, and Paciran MAWS, respectively.

### In-situ MHW Characteristic

The availability of in-situ data varies among the four locations: Patimban and Rembang have records starting from September 2022, while data for Karimunjawa and Paciran begin in September 2023 and October 2023, respectively (Figure 2). To ensure a fair comparison, the MHW characteristics from satellite data were analyzed only during the specific period of data availability for each corresponding in-situ station. The result show that satellite data generally detected a higher frequency of MHW events than the in-situ data, with the exception of Rembang. Interestingly, although the in-situ data at Patimban, Karimunjawa, and Paciran recorded fewer events, they often exhibited a higher number cumulative MHW days. This indicates that MHWs detected by in-situ sensors, while less frequent, were significantly longer in duration (Table 1). The different pattern observed at Rembang, where MHWs based in-situ data have a shorter duration than the satellite, is likely due to its distinct physical characteristics. Its shallower waters cause it to both heat up and cool down more rapidly.

In contrast, the maximum intensity of MHWs was typically higher in the in-situ records than in the satellite data. This is attributed to the ability of in-situ sensors to capture localized thermal peaks accurately, whereas the satellite's 0.05° spatial resolution averages these extreme over wider area, resulting in a smoothing effect that lowers the observed maximum intensity (Schlegel *et al.* 2017).

The performance of the satellite data was evaluated using the POD and FAR (Table 2), with the day by day event matching visualized in a timeline plot (Figure 3). Paciran exhibited the best performance with the highest POD (0.74) and a low FAR (0.13), which is visually represented in its timeline by significant overlap of Hit events (Figure 3d) and indicating strong agreement with

the in-situ observation despite having the shortest data record. While Karimunjawa also showed a low FAR (0.13), its lower POD (0.64) is attributable to several Miss events where the satellite failed to detect an in-situ MHW (Fig 3b) detection. In contrast, Patimban had a similar POD (0.66) but a significantly higher FAR (0.34), corresponding to numerous False Alarm events where the satellite identified MHWs not present in the in-situ record (Figure 3a).

We investigated the local drivers of MHWs at each station by calculating wind speed, Diurnal Temperature Range (DTR), and daily solar radiation accumulation for the available data period at each station. At Paciran station, a clear trigger pattern was observed as shown in Figure 5. Relationship between wind speed (Figure 5a) and total accumulated solar radiation (Figure 5c) exhibits a negative correlation or inverse relationship. Periods of low wind speed, typically around 2-4 m/s, often coincide with high daily total solar radiation accumulation (above 200 MJ/m<sup>2</sup>), particularly noticeable at the onset of each MHW event. This consistency suggests that calm wind condition are frequently associated with clear skies or reduced cloud cover, enabling the maximum net solar radiation flux to transmit to the sea surface (Kawai and Wada, 2007). A clear inverse relationship is observed between wind speed and DTR (Figure 5a and b). Periods of high DTR (peaking above 2°C), such as in March, August, and November 2024, tend to occur when wind speeds are low. Weak winds reduce vertical mixing in the water column, allowing heat from solar radiation to be trapped in a thin surface layer and produce a stable stratification (Bellenger and Duvel, 2009; Filipiak *et al.* 2012), known as the Diurnal Warm Layer (DWL). This phenomenon effectively increases the maximum sea surface temperature (SST<sub>max</sub>) during the day, resulting in a sharp increase in DTR.

**Tabel 1.** Comparison of Satelite and In-situ MHW Characteristics

Station	Frequency (Event)		Cumulative Days		Total Mean Duration (Days)		Maximum Intensity (°C)	
	Satellite	In-Situ	Satellite	In-Situ	Satellite	In-Situ	Satellite	In-Situ
Patimban	14	13	244	258	17.4	19.8	0.76	1.01
Karimunjawa	9	8	164	225	18.2	28.1	0.92	0.91
Rembang	6	18	202	191	33.7	10.6	0.69	1.08
Paciran	12	8	240	282	20.0	35.2	0.83	1.00

**Tabel 2.** Satellite Data Performance

Station	Hits (days)	Misses (days)	False Alarm (days)	POD	FAR
Patimban	171	87	89	0.66	0.34
Karimunjawa	143	82	21	0.64	0.13
Rembang	83	108	119	0.43	0.59
Paciran	209	73	32	0.74	0.13

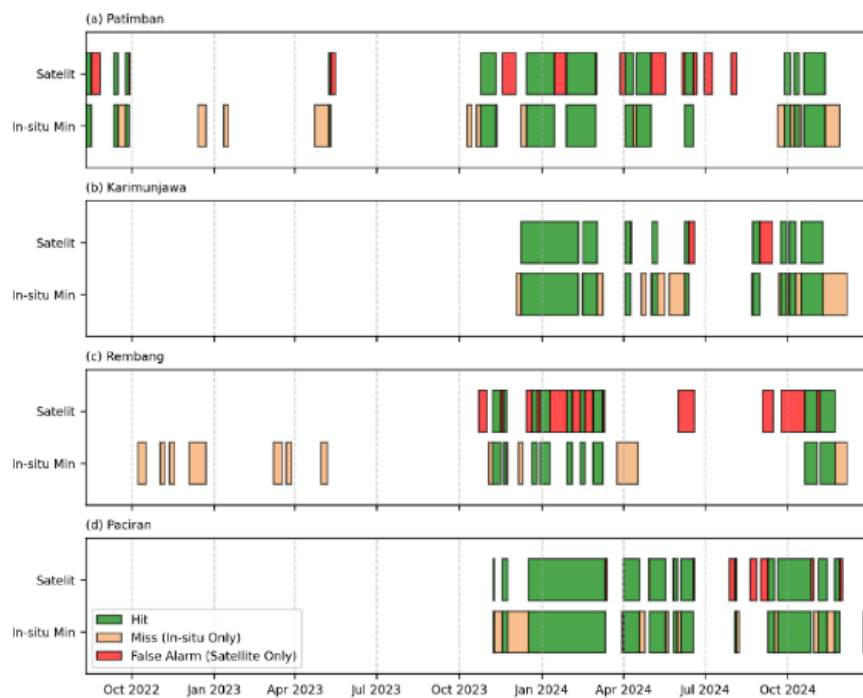


**Figure 4.** MHW event validation timeline comparing satellite and in-situ minimum temperature data for the (a) Patimban, (b) Karimunjawa, (c) Rembang, and (d) Paciran Stations. Green bars represent ‘Hits’ where both datasets detected an MHW, orange bars are ‘Misses’ where events were detected by in-situ sensor only, and red bars are ‘False Alarms’ detected by satellite only.

Overall, there is a strong positive correlation between high total accumulated solar radiation and high DTR in Paciran. The sharp increase in DTR in March and November 2024 was preceded or coincided with a surge in solar radiation, supported by relatively calm winds (Bellenger and Duvel, 2009). Solar radiation is the primary energy input that drives daily SST maximum. In other words, high daily net energy input will drive high DTR, provided that wind conditions support surface thermal stratification.

At Karimunjawa station, the local atmospheric and oceanic dynamics reveal a clear connection between wind speed, solar radiation, and DTR (Figure 6). Wind speed in Karimunjawa fluctuates moderately throughout the year, typically

ranging between 3–6 m/s, (Figure 6a) with lower values recorded during transition seasons April and November 2024. MHW events (shaded pink areas in Figure 6d) primarily occurred when wind speeds decreased and solar radiation accumulated increased above 180 MJ/m<sup>2</sup> (Figure 6b), particularly around November 2023–April 2024 and again during September–November 2024. These conditions favor enhanced solar radiation transmit into the surface ocean, coinciding with weak wind-driven mixing.

The amplitude DTR in Karimunjawa remained relatively low (mostly below 1°C) (Figure 6b), reflecting a more stable marine environment with stronger vertical mixing due to ocean-sea condition. This reduced DTR amplitude

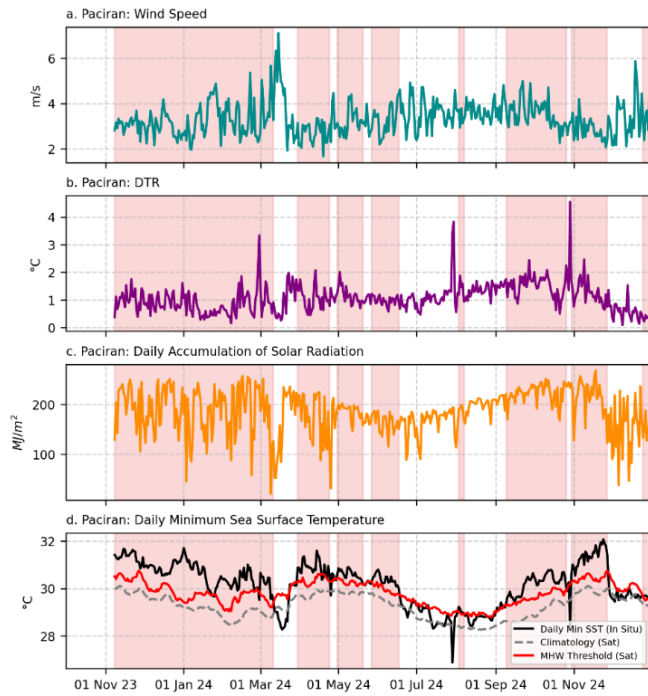


**Figure 5.** Time series of (a) daily mean wind speed, (b) Diurnal Temperature Range (DTR), (c) daily accumulation of solar radiation, and (d) sea surface temperature comparation from November 2023-Desember 2024 in Paciran Station. The shade pink areas indicate MHW periods detected from the daily minimum temperature.

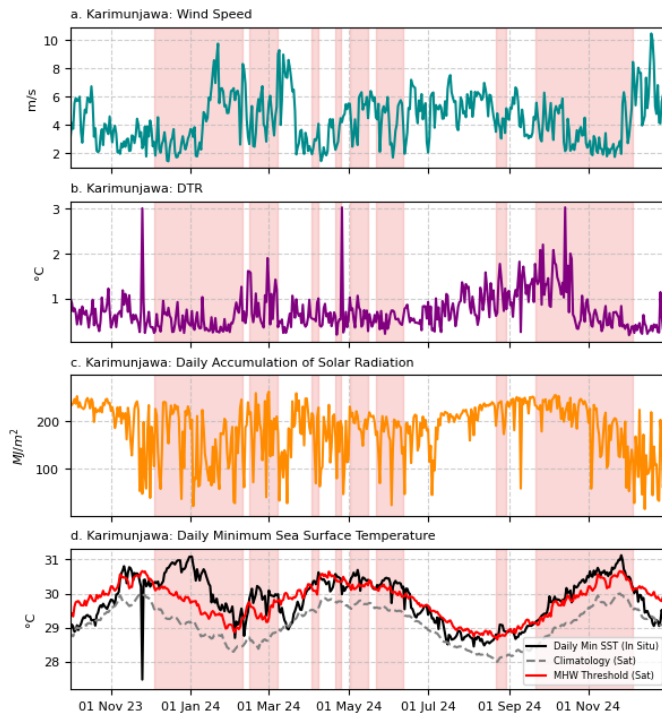


**Figure 6.** Time series of (a) daily mean wind speed, (b) Diurnal Temperature Range (DTR), (c) daily accumulation of solar radiation, and (d) sea surface temperature comparation from November 2023-Desember 2024 in Karimunjawa Station. The shade pink areas indicate MHW periods detected from the daily minimum temperature.

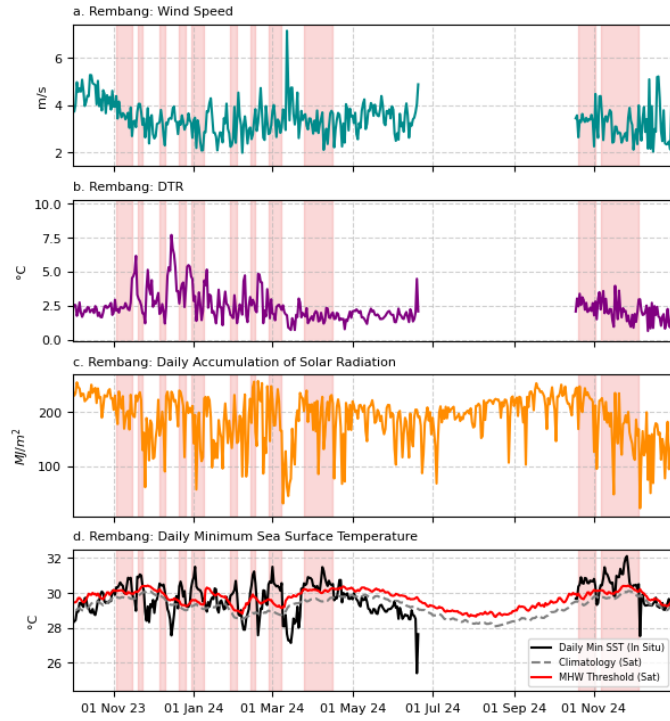


**Figure 7.** Time series of (a) daily mean wind speed, (b) Diurnal Temperature Range (DTR), (c) daily accumulation of solar radiation, and (d) sea surface temperature comparation from November 2023-Desember 2024 in Rembang Station. The shade pink areas indicate MHW periods detected from the daily minimum temperature.

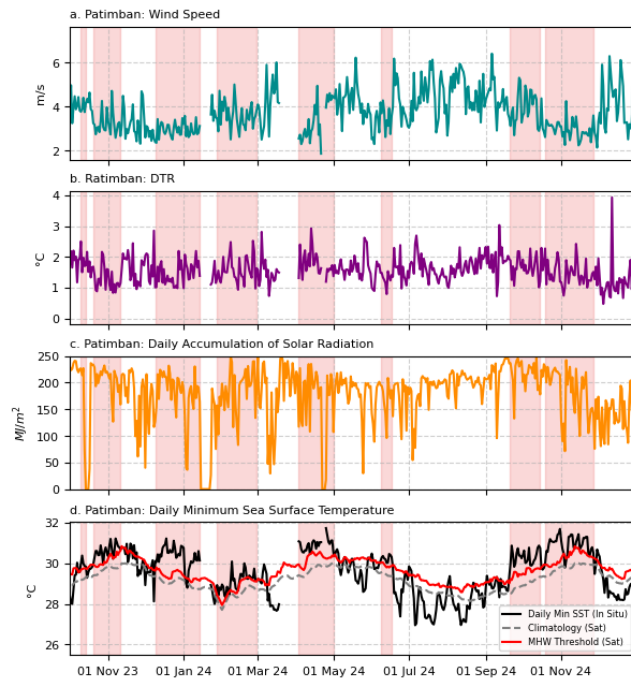


**Figure 8.** Time series of (a) daily mean wind speed, (b) Diurnal Temperature Range (DTR), (c) daily accumulation of solar radiation, and (d) sea surface temperature comparation from November 2023-Desember 2024 in Patimban Station. The shade pink areas indicate MHW periods detected from the daily minimum temperature.

suggest that although diurnal heating process exists, it is less efficient at forming a shallow diurnal warm layer (DWL) compared to coastal sites such as Paciran. Nevertheless, the synchronization between periods of weak winds, elevated solar radiation, and the MHW onset still highlights the important role of local diurnal heating in modulating thermal extremes, even in an environment where large scale atmospheric forcing strongly interacts with local radiative forcing.

At Rembang station, the temporal variability of local drivers shows a more distinct diurnal response and higher short term variability than at other location (Figure 7). MHW events occur primarily between November 2023 and May 2024, with additional shorter events toward the end of 2024. Wind speed display frequent fluctuations (2-6 m/s) (Figure 7a) and lower wind speed are often followed by increases in both solar radiation and DTR (Figure 7b-c). The DTR signal at Rembang is particularly strong, with frequent peaks above 3°C and several exceeding 5°C, indicating intense diurnal warming episodes.

Similar to Parcir, there is a clear inverse relationship between wind speed and DTR. Weak winds limit vertical mixing, allowing the formation of a shallow, strongly stratified surface layer. This promotes the accumulation of solar heat and supports the diurnal warm layer mechanism responsible for daytime SST amplification. Consequently, MHW onsets tend align with these calm, high radiation periods. However, the Rembang record also reveals numerous short lived MHWs, suggesting that system responds quickly to variations in local forcing possibly due to shallow bathymetry or river run off. In summary, Rembang describe a highly responsive coastal system where small scale fluctuations in wind and solar forcing can rapidly modify the sea surface thermal.

At Patimban station, a irregular relationship between atmospheric variables and MHW was observed as show in Figure 8. Relationship between wind speed (Figure 8a) and total accumulated solar radiation (Figure 8c) exhibits a negative correlation or inverse relationship. Wind speed remains moderate (3-5 m.s) for most of the year but exhibits episodic weakening during January and November 2024. Periods of low wind speed in January 2024, typically around 2-3 m/s, often coincide with high daily total solar radiation accumulation (above 200 MJ/m<sup>2</sup>), particularly noticeable at the onset of MHW event. This consistency suggests that calm wind condition are

frequently associated with clear skies or reduced cloud cover, enabling the maximum net solar radiation flux to transmit to the sea surface (Kawai and Wada, 2007). However, A clear inverse relationship is observed between wind speed and DTR (Figure 8a and b). Periods of high DTR (peaking above 2°C), such as in January, May, Oktober, and November 2024, tend to occur when wind speeds are low. Weak winds reduce vertical mixing in the water column, allowing heat from solar radiation to be trapped in a thin surface layer and produce a stable stratification (Bellenger and Duvel, 2009; Filipiak *et al.* 2012), known as the Diurnal Warm Layer (DWL). This phenomenon effectively increases the maximum sea surface temperature (SST<sub>max</sub>) during the day, resulting in a sharp increase in DTR. Exception condition occurs during December 2024, DTR shows spike exceeding 5°C, suggest transient and localized thermal instabilities likely driven by shallow coastal processes rather than consistent atmospheric control.

However, there is unclear correlation between total accumulated solar radiation and DTR. While periods of high solar radiation (> 180 MJ/m<sup>2</sup>) often overlap with weak wind conditions, DTR response is less systematic. This inconsisteny may arise from additional coastal influences such as tidal mixing, freshwater input from nearby river systems, and turbidity variation that alter local heat storage and surface energy balance. These factors likely contribute to a noisy DTR signal and a weaker correlation between surface heating and MHW onset. Despite these complexities, Patimban still exhibits the broader tendency for MHW events to occur during period of enhanced solar radiation and reduced wind speed. The weaker coupling between DTR radiation suggest that MHW formation here influenced not only by diurnal heating but also by mesoscale or coastal processes controlling vertical stratification.

Driver analysis reveals that MHW at all locations is influenced by local atmospheric drivers, namely wind and solar radiation, with varying responses. Paciran and Rembang show very strong and distinct diurnal patterns. When the wind is calm and solar radiation is high, this directly triggers a high DTR, indicating intense DWL formation. Karimunjawa shows the same diurnal triggers, but its DTR response is much weaker (below 1°C) due to open sea conditions that allow for stronger vertical mixing. Patimban shows

an irregular pattern. Although diurnal processes exist, the relationship between radiation and DTR is unclear and inconsistent, most likely confused by complex local coastal influences such as river inflow and tides.

## CONCLUSION

This study successfully detected and analyzed Marine Heatwave (MHW) events at four coastal stations on the north coast of Java and adjacent islands during the 2022–2024 period by combining in-situ data with satellite-derived climatologies. Although the in-situ records are relatively short, this study confirms their crucial value as a ground truth for revealing coastal phenomena that may not be fully captured by satellites. Spatial analysis indicates that MHWs with the highest maximum intensity occur in the open ocean, yet coastal regions experience a higher frequency of events and more cumulative MHW days. This suggests that the primary threat of coastal MHWs lies not in their peak intensity, but in their vulnerability to occur frequently and for prolonged durations. Direct comparison also shows that the maximum intensity from in-situ data is generally higher than that from satellites, likely due to the smoothing effect of the coarser spatial resolution of satellite data. Satellite performance validation reveals highly variable results, ranging from the best performance at Paciran (POD=0.74, FAR=0.13) to significant mismatches at other stations like Rembang. Driver analysis reveals that MHWs at all location is influenced by local wind and solar radiation with varying responses. Rembang and Paciran shows very strong and distinct diurnal patterns, while Karimunjawa shows lower diurnal pattern. Meanwhile, Patimban shows an irregular pattern likely confused by complex local coastal influence. This variability highlights the importance of local validation and the use of in-situ data for monitoring MHWs in Indonesia's dynamic coastal environments.

## REFERENCE

Beliyana, E., Ningsih, N.S., & Tarya, A. 2022. Characteristics of marine heatwaves (2008–2021) in the Savu Sea, East Nusa Tenggara. *Journal of Physics: Conference Series*, 2377(1): 012043. doi: 10.1088/1742-6596/2377/1/012043

Bellenger, H., & Duvel, J.-P. 2009. An analysis of tropical ocean diurnal warm layers. *Journal of Climate*, 22: 3629–3646. doi: 10.1175/2008JCLI2598.1

Chen, Y., Shen, C., Zhao, H., & Pan, G. 2024. The impact of marine heatwaves on surface phytoplankton chlorophyll-a in the South China Sea. *Science of the Total Environment*, 949: 175099. doi: 10.1016/j.scitotenv.2024.175099

Choi, H.-Y., Park, M.-S., Kim, H.-S., & Lee, S. 2024. Marine heatwave events strengthen the intensity of tropical cyclones. *Communications Earth & Environment*, 5: 69. doi: 10.1038/s43247-024-01239-4

Clayson, C.A., & Weitlich, D. 2007. Variability of tropical diurnal sea surface temperature. *Journal of Climate*, 20: 334–352. doi: 10.1175/JCLI3999.1

Donlon, C.J., Martin, M., Stark, J., Roberts-Jones, J., Fiedler, E., & Wimmer, W. 2012. The operational sea surface temperature and sea ice analysis (OSTIA) system. *Remote Sensing of Environment*, 116: 140–158. doi: 10.1016/j.rse.2010.10.017

Filipiak, M.J., Merchant, C.J., Kettle, H., & Le Borgne, P. 2012. An empirical model for the statistics of sea surface diurnal warming. *Ocean Science*, 8: 197–209. doi: 10.5194/os-8-197-2012

Frölicher, T.L., Fischer, E.M., & Gruber, N. 2018. Marine heatwaves under global warming. *Nature*, 560: 360–364. doi: 10.1038/s41586-018-0383-9

Hobday, A.J., Oliver, E.C.J., Sen Gupta, A., Benthuyzen, J.A., Burrows, M.T., Donat, M.G., Holbrook, N.J., Moore, P.J., Thomsen, M.S., Wernberg, T., & Smale, D.A. 2018. Categorizing and naming marine heatwaves. *Oceanography*, 31(2): 162–173. doi: 10.5670/oceanog.2018.205

Hobday, A.J., Alexander, L.V., Perkins, S.E., Smale, D.A., Straub, S.C., Oliver, E.C.J., Benthuyzen, J.A., Burrows, M.T., Donat, M.G., Feng, M., Holbrook, N.J., Moore, P.J., Scannell, H.A., Sen Gupta, A., & Wernberg, T. 2016. A hierarchical approach to defining marine heatwaves. *Progress in Oceanography*, 141: 227–238. doi: 10.1016/j.pocean.2015.12.014

Holbrook, N.J., Scannell, H.A., Sen Gupta, A., Benthuyzen, J.A., Feng, M., Oliver, E.C.J., Alexander, L.V., Burrows, M.T., Donat,

M.G., Hobday, A.J., Moore, P.J., Perkins-Kirkpatrick, S.E., Smale, D.A., Straub, S.C., & Wernberg, T. 2019. A global assessment of marine heatwaves and their drivers. *Nature Communications*, 10: 2624. doi: 10.1038/s41467-019-10206-z

Iskandar, M.R., Ismail, M.F.A., Arifin, T., & Chandra, H. 2021. Marine heatwaves of sea surface temperature off south Java. *Heliyon*, 7: e08618. doi: 10.1016/j.heliyon.2021.e08618

Jones, T., Parrish, J.K., Peterson, W.T., Bjorkstedt, E.P., Bond, N.A., Ballance, L.T., Bowes, V., Hipfner, J.M., Burgess, H.K., Dolliver, J.E., Lindquist, K., Lindsey, J., Nevins, H.M., Robertson, R.R., Roletto, J., Wilson, L., Joyce, T., & Harvey, J. 2018. Massive mortality of a planktivorous seabird in response to a marine heatwave. *Geophysical Research Letters*, 45: 3193–3202. doi: 10.1029/2017GL076164

Kawai, Y., & Wada, A. 2007. Diurnal sea surface temperature variation and its impact on the atmosphere and ocean: A review. *Journal of Oceanography*, 63: 721–744. doi: 10.1007/s10872-007-0063-0

Maulida, T., Wirasatriya, A., Ismunarti, D.H., & Puryajati, A.D. 2022. Physical drivers of the 2013 marine heatwave in the seas of the southern Java–Nusa Tenggara. *Geographia Technica*, 17: 129–139. doi: 10.21163/GT\_2022.171.10

Mazzini, P.L.F., & Pianca, C. 2022. Marine heatwaves in the Chesapeake Bay. *Frontiers in Marine Science*, 8: 750265. doi: 10.3389/fmars.2021.750265

Oliver, E.C.J., Benthuyzen, J.A., Darmaraki, S., Donat, M.G., Hobday, A.J., Holbrook, N.J., Schlegel, R.W., & Sen Gupta, A. 2021. Marine heatwaves. *Annual Review of Marine Science*, 13: 313–342. doi: 10.1146/annurev-marine-032720-095144

Oliver, E.C.J., Donat, M.G., Burrows, M.T., Moore, P.J., Smale, D.A., Alexander, L.V., Benthuyzen, J.A., Feng, M., Sen Gupta, A., Hobday, A.J., Holbrook, N.J., Perkins-Kirkpatrick, S.E., Scannell, H.A., Straub, S.C., & Wernberg, T. 2018. Longer and more frequent marine heatwaves over the past century. *Nature Communications*, 9: 1324. doi: 10.1038/s41467-018-03732-9

Pearce, A. 2011. The marine heat wave off Western Australia during the summer of 2010/11. *Journal of Marine Systems*, 111–112: 139–156. doi: 10.1016/j.jmarsys.2012.10.009

Roebber, P.J. 2009. Visualizing multiple measures of forecast quality. *Weather and Forecasting*, 24: 601–608. doi: 10.1175/2008WAF2222159.1

Sato, H., Takemura, K., Ito, A., Umeda, T., Maeda, S., Tanimoto, Y., Nonaka, M., & Nakamura, H. 2024. Impact of an unprecedented marine heatwave on extremely hot summer over northern Japan in 2023. *Scientific Reports*, 14: 16100. doi: 10.1038/s41598-024-65291-y

Schlegel, R.W., Oliver, E.C.J., Wernberg, T., & Smit, A.J. 2017. Nearshore and offshore co-occurrence of marine heatwaves and cold-spells. *Progress in Oceanography*, 151: 189–205. doi: 10.1016/j.pocean.2017.01.004

Smale, D.A., Wernberg, T., Oliver, E.C.J., Thomsen, M.S., Harvey, B.P., Straub, S.C., Burrows, M.T., Alexander, L.V., Benthuyzen, J.A., Donat, M.G., Feng, M., Hobday, A.J., Holbrook, N.J., Perkins-Kirkpatrick, S.E., Scannell, H.A., Sen Gupta, A., Payne, B.L., & Moore, P.J. 2019. Marine heatwaves threaten global biodiversity and the provision of ecosystem services. *Nature Climate Change*, 9: 306–312. doi: 10.1038/s41558-019-0412-1